Cerebral Cortex, February 2020;30: 550–562

doi: 10.1093/cercor/bhz106
Advance Access Publication Date: 20 June 2019
Original Article

ORIGINAL ARTICLE

Translating Fear Circuitry: Amygdala Projections to Subgenual and Perigenual Anterior Cingulate in the Macaque

K. K. Sharma[1,†], E. A. Kelly[1,†], C. W. Pfeifer[1] and J. L. Fudge[1,2]

[1]Department of Neuroscience and [2]Department of Psychiatry, School of Medicine and Dentistry, University of Rochester, Rochester, NY 14642, USA

Address correspondence to: Julie L. Fudge, Departments of Neuroscience and Psychiatry, The Del Monte Institute for Neuroscience, University of Rochester Medical Center, 601 Elmwood Avenue, Box 603 Rochester, NY 14642, USA. Email: julie_fudge@urmc.rochester.edu.

[†]These authors contributed equally to this work

Abstract

Rodent fear-learning models posit that amygdala–infralimbic connections facilitate extinction while amygdala–prelimbic prefrontal connections mediate fear expression. Analogous amygdala–prefrontal circuitry between rodents and primates is not established. Using paired small volumes of neural tracers injected into the perigenual anterior cingulate cortex (pgACC; areas 24b and 32; a potential homologue to rodent prelimbic cortex) and subgenual anterior cingulate cortex (sgACC, areas 25 and 14c; a potential homologue to rodent infralimbic cortex) in a single hemisphere, we mapped amygdala projections to the pgACC and sgACC within single subjects. All injections resulted in dense retrograde labeling specifically within the intermediate division of the basal nucleus (Bi) and the magnocellular division of the accessory basal nucleus (ABmc). Areal analysis revealed a bias for connectivity with the sgACC, with the ABmc showing a greater bias than the Bi. Double fluorescence analysis revealed that sgACC and pgACC projections were intermingled within the Bi and ABmc, where a proportion were double labeled. We conclude that amygdala inputs to the ACC largely originate from the Bi and ABmc, preferentially connect to the sgACC, and that a subset collaterally project to both sgACC and pgACC. These findings advance our understanding of fear extinction and fear expression circuitry across species.

Key words: fear conditioning, anterior cingulate, prelimbic, infralimbic, accessory basal

Introduction

Connections between the anterior cingulate and amygdala are of critical interest in the study of fear learning, fear extinction, and disorders of emotional regulation (Maren and Quirk 2004; Quirk and Mueller 2008; Giustino and Maren 2015; Likhtik and Paz 2015). A circuit model, originating from rodent studies, posits that infralimbic cortex (IL) activity during extinction decreases fear expression and facilitates the consolidation of extinction memories, while activity in the prelimbic cortex (PL) contributes to both fear acquisition and retrieval (Vidal-Gonzalez et al. 2006; Burgos-Robles et al. 2007; Burgos-Robles et al. 2009; Sierra-Mercado et al. 2011). In larger species, the proposed analogues of the IL and PL are located in the anterior cingulate cortex (ACC), and functional neuroimaging studies in human fear conditioning indicate a similar dichotomy. The activity in the human subgenual ACC (sgACC), corresponding to the IL, is correlated with extinction memory strength (Phelps et al. 2004; Schiller and Delgado 2010; Etkin et al. 2011), and the activity in more dorsal anterior cingulate sectors is generally

correlated with fear expression (Milad et al. 2007b; Etkin et al. 2011). More recently, Senn et al. (2014) optogentically manipulated specific amygdala–PFC circuits during extinction training in mice and found that inhibition of amygdala–IL projections reduced the efficacy of the extinction memory while inhibition of amygdala–PL projections increased the efficacy. These studies provide strong evidence that amygdala–IL connections are critical to extinction memory formation while amygdala–PL connections mediate fear potentiation. However, fear extinction and anatomical studies in rodents have not directly compared IL and PL projections of the amygdala within the same animal (Matyas et al. 2014; Senn et al. 2014; Klavir et al. 2017; Marek et al. 2018). Moreover, the specific connectivity between the amygdala and these anterior cingulate subdivisions is incompletely explored in the macaque, where cortical anatomy closely resembles that in humans. Understanding the topography of these connections is a critical step in translating fear circuitry from rodents to humans.

The IL roughly corresponds to the primate areas 25 and 14c and the PL to the areas 32 and 24. Across species, these subregions share a general set of local and long-range connections (Krettek and Price 1977; Sesack et al. 1989; Ongur and Price 2000; Heilbronner et al. 2016). Cross-species studies of cytoarchitecture (Vogt and Paxinos 2014) and subcortical connectivity (Ongur and Price 2000; Heilbronner et al. 2016) endorse homology between the IL and the sgACC (specifically, area 25). These findings are corroborated by functional neuroimaging studies of human fear extinction that implicate sgACC activity in the process of extinction memory formation (Phelps et al. 2004; Schiller and Delgado 2010; Etkin et al. 2011), which matches the role of the IL in functional studies in rodents (Vidal–Gonzalez et al. 2006; Burgos-Robles et al. 2007; Sierra-Mercado et al. 2011; Senn et al. 2014). The correlate of the murine PL is less well established. Cytoarchitecture and connectional analysis across species posit that area 32 is the true homolog of the PL (Vogt et al. 2013); however, the evolutionary expansions and increased laminar differentiation of area 32 between rodents and primates impede the ability to specifically attribute analogous function to homologous regions (Dombrowski et al. 2001; Ongur et al. 2003; Wise 2008). For example, in primates, area 24a is interposed between areas 25 and 32, while area 24b is caudally adjacent to area 32 only. In rodents the situation is somewhat more straightforward with area 24a caudally contiguous with areas 25 and 24b caudally contiguous with area 32, according to recent atlases (e.g. Vogt and Paxinos 2014) (see Discussion in Supplementary Material). Owing to the lack of resolution inherent in neuroimaging studies, the region encompassing areas 24/32 is called the perigenual ACC (pgACC) in human studies. Elucidating specific pathways and differential connectivity between the amygdala, "sgACC", and "pgACC" in the macaque may further our understanding of possible homologies between rodents and primates.

The amygdala and ACC are extensively connected in rodents and in the macaque (Price et al. 1987; McDonald 1991a; McDonald 1998). In rats and mice, amygdala–ACC projections largely originate from the lateral and basolateral nuclei (BLA) (Krettek and Price 1977; McDonald 1991a; Hoover and Vertes 2007; Senn et al. 2014). In rats, a subset of amygdala–ACC projections collaterally project to the lateral prefrontal cortex (Sarter and Markowitsch 1984). In the macaque, projections from the amygdala terminate within the ACC with a very high density, in addition to other cortical regions (Amaral and Price 1984; Barbas and de Olmos 1990; Carmichael and Price 1996; Aggleton et al. 2015). Projections to the primate ACC originate from the basal nucleus (the "basolateral" nucleus in rodents) and accessory basal nucleus (AB) of the amygdala, with notably minimal direct input from the lateral nucleus (Amaral and Price 1984; Price et al. 1987; Barbas and de Olmos 1990; Carmichael and Price 1996; Aggleton et al. 2015) (see Supplementary Figure 1 and Supplementary Discussion for amygdala neuroanatomy). The posterior division of the rodent basomedial nucleus (BMAp), which is the murine counterpart to the AB (Krettek and Price 1978; Petrovich et al. 1996), is often absent from circuit investigations of the rodent amygdala (Giustino and Maren 2015). The specifics of BMAp and AB connectivity with the ACC are highly relevant to translating fear circuitry because the AB constitutes an evolutionarily expanded nucleus of the primate amygdala in both macaques and humans (Stephan et al. 1987; Amaral et al. 1992) and may transmit information relevant to extinction (Adhikari et al. 2015).

Given the overall expansion of the amygdala and ACC in humans (Wise 2008; Petrides et al. 2012), we thought it pertinent to establish the connections between specific amygdala nuclei and specific subregions of the ACC in the macaque to increase our understanding of how rodent fear circuitry maps onto higher species. While previous monkey studies have examined general amygdala–ACC connectivity (Porrino et al. 1981; Amaral and Price 1984; Barbas and de Olmos 1990; Ghashghaei and Barbas 2002; Aggleton et al. 2015), we sought to compare the topography of putative "extinction"-associated paths (areas 25/14c) and "fear amplification" paths (areas 24/32) in the same animal using relatively small injections. To investigate this, we varied the locations of paired injections of retrograde tracers into area 25 and/or 14c (sgACC) and area 32 or 24b (pgACC) in a single hemisphere in the macaque and produced a map to directly compare amygdala projections to both regions in the same animal. Because some murine fear-learning models suggest relatively segregated microcircuits from the amygdala to the IL and PL (Vidal-Gonzalez et al. 2006; Sierra-Mercado et al. 2011; Senn et al. 2014; Giustino and Maren 2015; Burgos-Robles et al. 2017) despite evidence for collateral projections from limbic to prefrontal regions in rats (Sarter and Markowitsch 1984; McDonald 1991b), we also assessed the extent of collateral projections to the sgACC and pgACC in the macaque.

Materials and Methods

Design

The overall purpose of our study was to determine specific amygdala inputs to putative "homologues" of the IL and PL in monkeys (i.e. areas 25/14c and areas 24b/32, respectively). We designated injections that involved Brodmann areas 25 and/or 14c as sgACC and injections into areas 32 or 24b as perigenual anterior cingulate (pgACC). Area 14c was included in our definition of the sgACC due to its proximity with and cytoarchitectural and connectional similarity to area 25 (Carmichael and Price 1996). Detailed methods are provided in the Supplementary Methods. Briefly, we placed a small injection of a different bi-directional and/or retrograde tracer into the sgACC and pgACC of the same hemisphere in the macaque (*Macaque fascicularis*). Following sectioning and processing of the brain for tracers using immunocytochemistry, we mapped the distribution of retrogradely labeled cells in specific amygdala subregions. When retrogradely labeled cells from an injection pair were localized within the same amygdala region, we

conducted additional experiments to determine the proportion of double-labeled cells in the region, analyzing this in terms of specific paths, to understand the extent to which inputs to the sgACC or pgACC were segregated or shared.

Statistical Analysis

For the analysis of rostrocaudal and areal trends in amygdala–cortical projections, a total cell count for each injection site was summed across the rostrocaudal extent of the regions of interest (ROIs) determined from mapped sections. Injection sites were given an anterior–posterior value derived from mapping injections onto a common brain matched for species, age, and weight. Areal sums, analysis of variance (ANOVA) for cell count by tracer type, and linear regressions between injection site anterior–posterior value and cell counts were performed and scripted from raw data using R (R Foundation for Statistical Computing; http://www.R-project.org/).

For double-labeling studies, statistical analysis was performed using Prism VI statistical analysis software (GraphPad Software, Inc.). Within each z-projection image (see Supplementary Methods), the number of single-tracer filled cells (both channels collected separately) and dual-labeled cells was recorded for each ROI within each case. Cell counts were then normalized to reflect a ratio of projections to each injection site (area 25/14c, area 24/32, or dual) from the basal nucleus ROI and ABmc ROI in each animal. A 2×3 two-way ANOVA was performed on the means of these ratios to determine the dependence of projection ratio on ROI and injection site. Post hoc testing was conducted using Tukey's multiple comparison test (Tukey's HSD). A student's *t*-test (unpaired) was used when comparing 2 sample means. $P < 0.5$ was deemed statistically significant. Error bars are presented as standard error of the mean.

Results

Injection Sites and Cell Counts

A total of 17 bi-directional tracer injections were targeted to the sgACC and pgACC (Fig. 1*A–D*). In the sgACC, 3 injections were exclusively within area 25, 3 were in areas 25 and 14c, and 3 were exclusively within area 14c. In the pgACC, 4 injections were exclusively within area 24b, and 4 injections were within area 32, 2 of which also encroached on area 10 (Table 1). In aggregate, 9 pairs of injections were made such that 1 was in the sgACC (areas 25 and/or 14c) and the other in the pgACC (area 24b or 32) in the same hemisphere of an animal. In general, areas 14c/25, 24, and 32 express progressively increasing laminar differentiation moving from the sgACC to pgACC (Dombrowski et al. 2001; Ongur et al. 2003) and were identified by their established cytoarchitectonic features (e.g. Fig. 1*E*).

Projections from Amygdala to sgACC and pgACC Originate in the Intermediate Basal Nucleus and Magnocellular Accessory Basal Nucleus

In contrast to previous studies employing large injections encompassing multiple regions of the ventromedial prefrontal cortex, our confined injections allowed examination of a specific distribution of labeled cells within each nucleus of the amygdala. Additionally, paired injections targeting area 25 or 14c and area 32 or 24b allowed us to compare projection profiles from the amygdala in the same hemisphere. Using immunohistochemical staining and Neurolucida slide tracing software (see Supplemental Methods), we created maps of the distribution of retrograde-labeled cells in the amygdala projecting to each injection site (Fig.2; Supplementary Figure S1). In all 9 injection pairs, we consistently found that the most concentrated population of retrogradely labeled cells was in the intermediate basal nucleus (Bi) and the magnocellular division of the accessory basal nucleus (ABmc). Remarkably, other amygdala subregions had relatively few labeled cells. There were occasional labeled cells in the lateral nucleus and the periamygdaloid cortex, but these findings were not consistent across cases. This pattern of concentrated cell labeling in the Bi and ABmc held true regardless of the rostrocaudal locations of injection pairs in the ACC (e.g. Fig. 2*A* and *B*). Another consistent observation was intermingling of labeled cells resulting from each retrograde injection pair in both Bi and ABmc.

Anterograde Confirmation of Bi Projections

To confirm that the Bi is a source for projections to the sgACC and pgACC, we examined anterograde projections of tracers placed exclusively in the Bi using sections from a previous data set (Cho YT et al. 2013). In 2 male monkeys, injections restricted to the Bi (Fig. 3*A*) showed many labeled fibers in areas 32, 24, 25, and 14c (Fig. 3*B–D*), which terminated in superficial layers 2 and 3 as well as deep layer 5, consistent with previous findings (Morecraft et al. 2007). In contrast, analysis of 4 injections in other basal nucleus subregions, 2 in the magnocellular division of the basal nucleus (Bmc) and 2 in the parvocellular division of the basal nucleus (Bpc), revealed fiber labeling mainly in orbital, insular, and lateral prefrontal cortex with lower densities of labeled fibers in the ACC. Bmc and Bpc injections that resulted in labeled fibers in any one of areas 32, 24, 25, or 14c did not express fiber labeling in the whole set of areas (data not shown).

sgACC Receives More Amygdala Input Than pgACC

We next investigated whether projections from the amygdala formed a rostrocaudal gradient in the ACC, by matching each injection site to an anterior–posterior level in a prototypical brain matched for species, age, and weight and correlating injection cell counts with anterior–posterior position. Retrogradely labeled cell counts were restricted to totals within the ROIs established as main sources (ABmc and Bi; Fig.2). The total of labeled cells within the Bi and ABmc was significantly correlated with anterior–posterior position of the injection site (Slope = −7.3 cells/mm, $P = 0.033$, $R^2 = 0.221$, df = 15), indicating that inputs from these nuclei decreased from caudal to rostral within the ACC (Fig. 4*A*, Table 1). Multiple regression analysis of caudo–rostral trends for the Bi and ABmc revealed that both sets of labeled cells decreased from caudal to rostral and did not significantly differ in the rate of decrease (Fig. 4*B*; Slope = −3.7 cells/mm, $P = 0.005$, $R^2 = 0.199$, df = 32; Nucleus of Origin n.s., $P = 0.917$; Interaction of Nucleus of Origin and AP coordinate n.s., $P = 0.859$). Inspection of the data indicates that the numbers of labeled cells steadily decreased based on caudal–rostral position of the injection site even within subregions (Table 1), indicating a true pattern of innervation rather than inadvertent variation due to injection size or tracer. To investigate areal differences in connectivity, the total quantities of retrogradely labeled cells in the Bi and ABmc from injections in the sgACC and pgACC were plotted and compared. The sgACC injections resulted in substantially more retrogradely

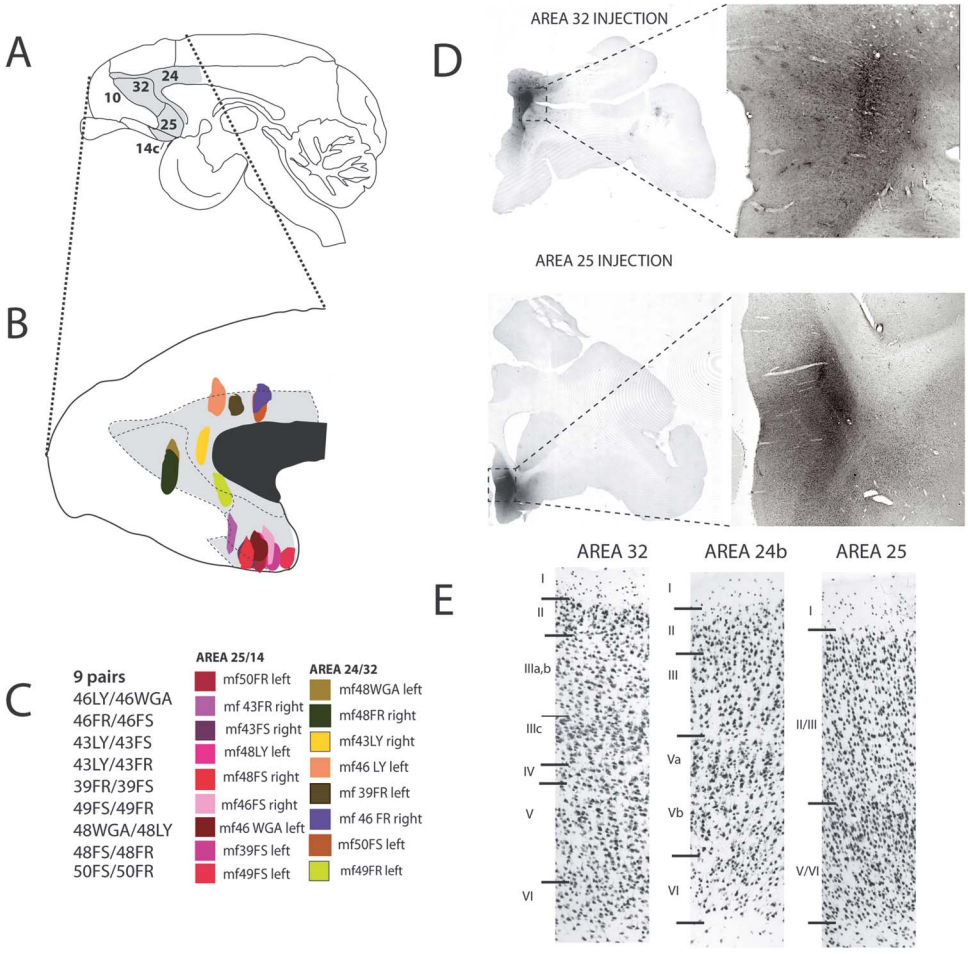

Figure 1. Brodmann area locations of paired injections across the sgACC and pgACC. (*A*) Sagittal schematic of Brodmann areas 25, 32, 24, 10, and 14c in the nonhuman primate brain. (*B*) Magnified (from *A*), a color-coded map of injection site locations. (*C*) Summary of injection pairs. A total of 9 pairs of retrograde tracer injections were made across the sgACC and pgACC of 6 male macaques (*Macaca fascicularis*). An injection in area 25 or 14c was paired with an injection in area 24b or 32 in the same hemisphere of the same individual animal. (*D*) Brightfield images of anti-tracer immunohistochemistry (IHC) (see Supplementary Methods), used for localization of injection sites. (*E*) Photomicrographs denoting the cytoarchitectonic differences in cortical layer thickness characteristic of each Brodmann area. Areas 32 and 24 are dysgranular with area 32 having a much larger Layer V. In contrast, area 25 is agranular (without a Layer IV). Area 14c shares a high degree of cytoarchitectural and connectional similarity with area 25 (Carmichael and Price 1996).

labeled cells than pgACC injections. Although each injection site location resulted in proportionately more labeled cells in the Bi compared with the ABmc, the sgACC injections stood out by having a relatively greater proportion of labeled cells in the ABmc compared with pgACC injections (Fig. 4C; pgACC: $n = 8$, 101 cells in Bi [73.9%], 36 cells in ABmc [26.1%]; sgACC: $n = 9$, 431 cells in Bi [52.1%], 396 cells in ABmc [47.8%]). This indicates differing contributions of the ABmc and Bi to the sgACC and pgACC, with sgACC receiving a greater contribution from the ABmc compared with the pgACC. To determine whether individual tracer properties influenced this finding, we examined the possibility of a correlation between tracer type and number of labeled cells across all injections and found none (ANOVA Cell Count × Tracer: $F = 1.498$, $P = 0.262$, df = 3).

Collateral Projections from the Amygdala to pgACC and sgACC

The intermingling of retrogradely labeled cells in both the ABmc and Bi from paired injections observed in Figure 2 suggests the possibility of a population of cells that collaterally project to the pgACC and sgACC. Using fluorescence immunocytochemistry for cases with paired sgACC/pgACC injections, we analyzed both populations of retrogradely labeled cells in the same section, through the entire rostrocaudal extent of the amygdala. We first collected low magnification images of neighboring sections stained with acetylcholinesterase (AChE) and carefully demarcated Bi and ABmc boundaries (Fig. 5A; Supplementary Methods). These measurements were then applied to adjacent fluorescently stained images, with careful alignment of landmarks (Fig. 5B). A 20× tile scan was collected from each amygdala ROI (Bi and ABmc) for 2 channels of fluorescence excitation, each one corresponding to a single tracer from either the pgACC or sgACC (Fig. 5C). Each fluorescence channel was acquired independently, such that 2 tile scans were produced for each ROI with z plane acquisition through the full depth of the section. Cells were counted independently within each tile scan, and scans were overlaid to identify cells marked with tracers from the pgACC and sgACC (Fig. 5D–F).

Table 1 Injection cell counts and cortical locations

Injection	Cells in ABmc and Bi	Areas 32 and 10	Area 32	Area 24b	Area 25	Areas 25 and 14	Area 14
48FR	0	+					
48WGA	0	+					
49FR	16		+				
43LY	41		+				
46FR	16			+			
50FS	35			+			
39FR	10			+			
46LY	18			+			
43FR	142				+		
50FR	50				+		
49FS	143				+		
43FS	84					+	
48LY	48					+	
46FS	230					+	
48FS	42						+
46WGA	41						+
39FS	47						+

A total of 17 injections in various subregions of the ACC. A "+" demarks the areal location of the injection. Injections with a "+" in areas 32 and 10 or areas 25 and 14 had injections partially in both areas. Cell counts represent the total number of cells counted through the rostrocaudal extent of the ABmc and basal nucleus. Cell counts did not correlate with the type of tracer injected ($F = 1.498$, $P = 0.262$). ABmc = magnocellular division of the accessory basal nucleus, Bi = intermediate division of the basal nucleus of the amygdala.

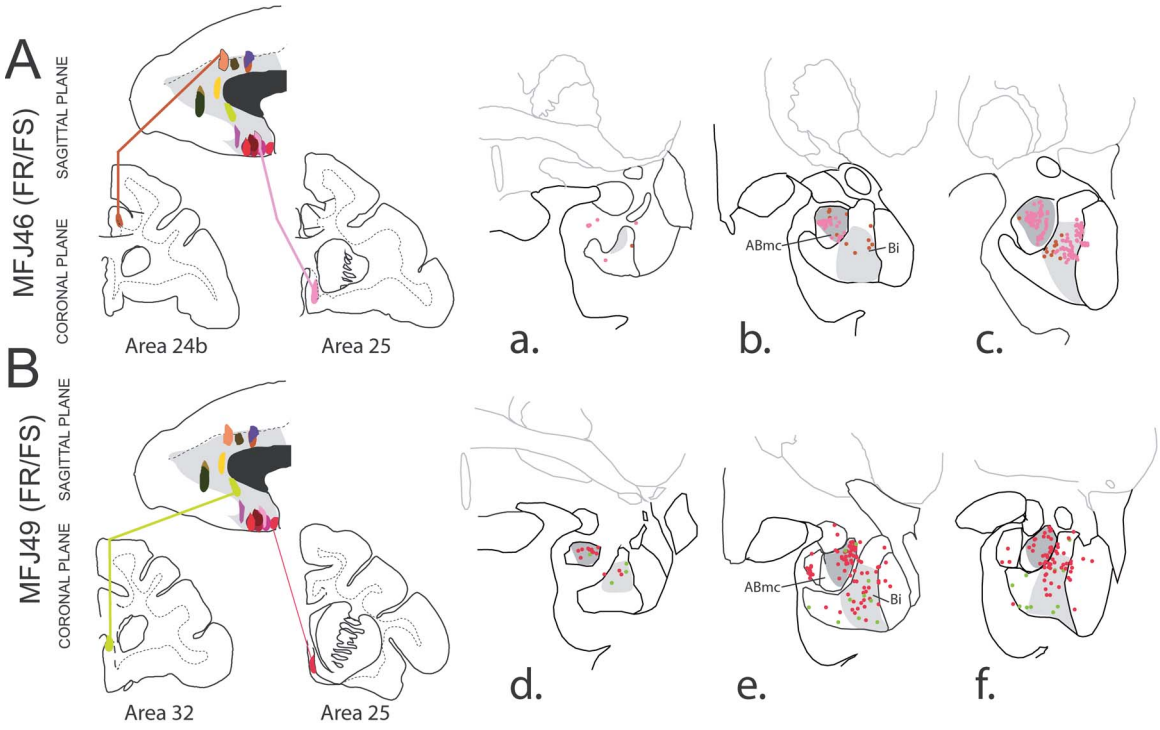

Figure 2. Regional-specific distribution of amygdala output neurons to the sgACC and pgACC. Maps of retrogradely labeled cells in the amygdala from paired neural tracer injections in Brodmann area 25 or 14c and area 32 or 24 were constructed. Left side of both case panels: sagittal plane diagram depicts all injections sites from our cases (Fig. 1B) with lines indicating the specific locations of the paired injections (coronal slices underneath) for the case. Right side of both panels: coronal wireframe maps of traced cell locations are provided from rostral to caudal through the amygdala (see Supplementary Figure S1 for anatomical reference). Black lines depict borders of amygdala subnuclei and tissue slice. Gray lines depict a variety of subcortical landmarks including the caudate, putamen, globus pallidus, and anterior commissure. (*A*) The locations of retrogradely labeled cells from injections in rostral area 25 (pink) and area 24 (dark orange) through the extent of the amygdala in case MFJ46. Note that almost all traced cells from both regions were confined to the Bi or the ABmc. (*B*) The locations of retrogradely labeled cells from injections in caudal area 25 (red) and area 32 (green) in case MFJ49. While more disperse than (*A*), the case in panel (*B*) shows the highest concentrations in the Bi and ABmc. Bi and ABmc nuclei labeled in 2B and 2E panels only to avoid figure crowding. Paired injections were made and analyzed within the same hemisphere.

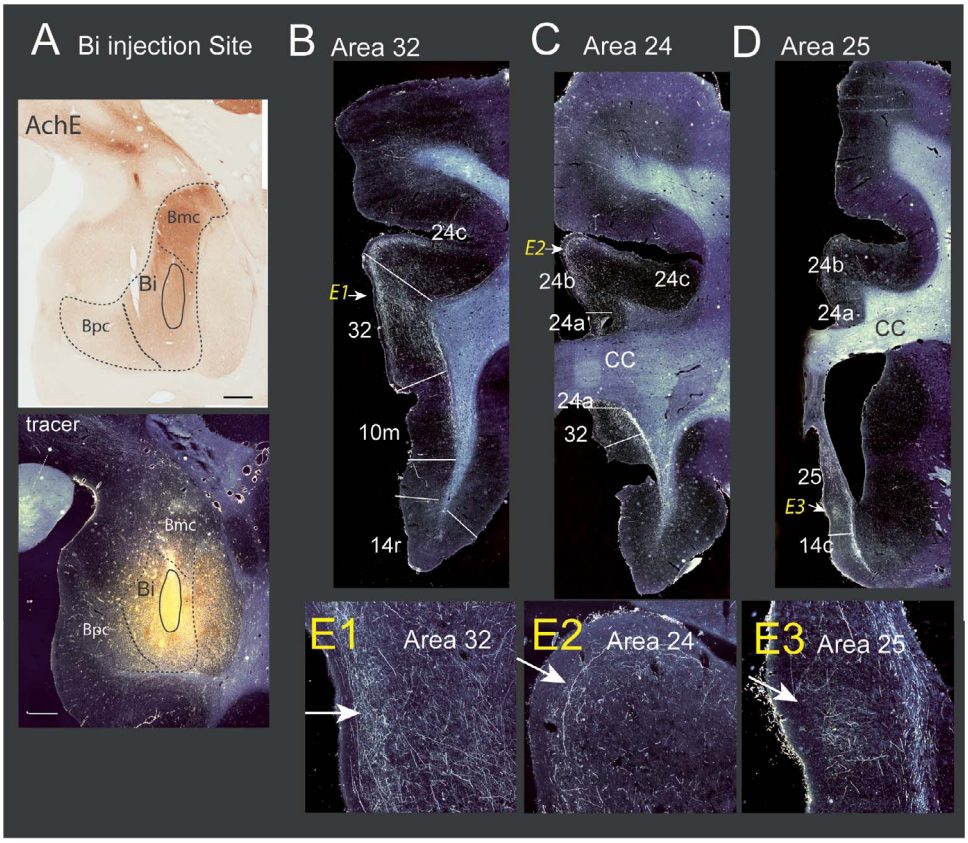

Figure 3. Anterograde fibers from intermediate basal nucleus project to Brodmann areas 32, 24, 25 (*A*) Top panel: visualization of amygdala subnuclei produced by acetylcholinesterase staining. Bottom panel: the injection site of neuronal tracer Lucifer yellow (LY) in the Bi. The black circle demarcates the localization of the injection. (*B–E*) Darkfield photomicrographs confirming projections from the Bi to areas 32 (*B*), 24b (*C*), 25 (*D*). (*B*) LY stained terminals present in Layer II (arrow; magnified in E1) of area 32. (*C*) LY staining superficial layers of area 24b (arrow; magnified in E2). (*D*) Terminals in superficial layers of area 25 (arrow; magnified in E3), which are mirrored in area 14c.

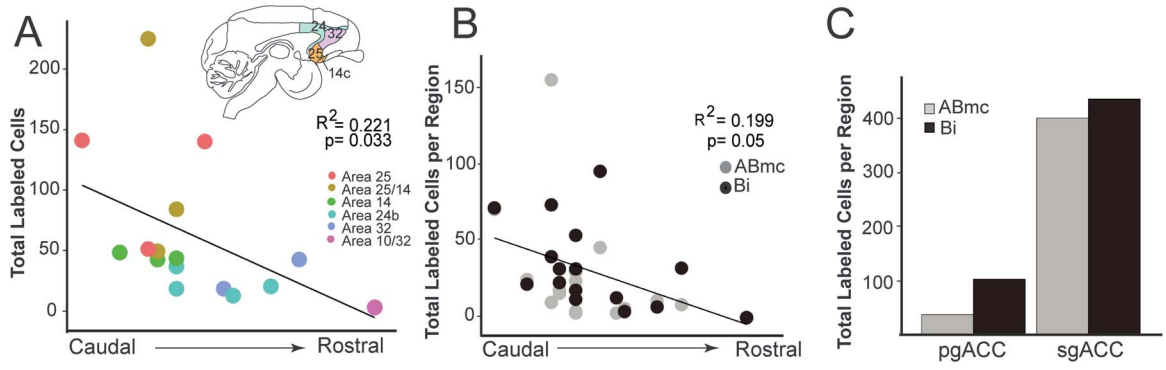

Figure 4. The subgenual anterior cingulate receives more input from the amygdala and a higher proportion of input from the ABmc. Injections sites were assigned coordinates according to their locations along the anterior–posterior axis in a standard brain matched for species, age, and weight. (*A*) Total labeled cells retrogradely labeled within the Bi and ABmc plotted in relation to the anterior–posterior position of the injection site. Sites are colored by their localization (Table 1). Overall inputs from the amygdala are increased caudally and decreased rostrally ($P = 0.033$, $R^2 = 0.221$). The schematic in the upper right illustrates the rostrocaudal relationships between Brodmann areas. Areas 25 and 14c constituted the most caudal injection sites in our data set. (*B*) Inputs from both the Bi and ABmc increased caudally ($P = 0.005$, $R^2 = 0.199$), and multiple regression revealed no differences in slope or total count between the two nuclei (Nucleus of Origin n.s., $P = 0.875$; Interaction of Nucleus of Origin and AP coordinate n.s., $P = 0.766$). (*C*) The total number of retrogradely labeled cells found in Bi and ABmc for all injections that were localized to the pgACC ($n = 8$, 101 cells in Bi [73.9%], 36 cells in ABmc [26.1%]) or sgACC ($n = 9$, 431 cells in Bi [52.1%], 396 cells in ABmc [47.8%]).

We first analyzed the average proportion of labeled cells in the Bi (Fig. 6A and B) and ABmc (Fig. 6C and D) that resulted from all sgACC (area 25/14c) and pgACC (area 24b/32) injections. A significantly greater proportion of single-labeled cells in Bi were found following injections in area 25/14c (55.81%, Fig. 6A; 61.38 mean cell count per injection, Fig. 6B) when compared with injections in area 24b/32 (35.11%; 38.62 mean cell count per injection). In addition, there was a subpopulation of

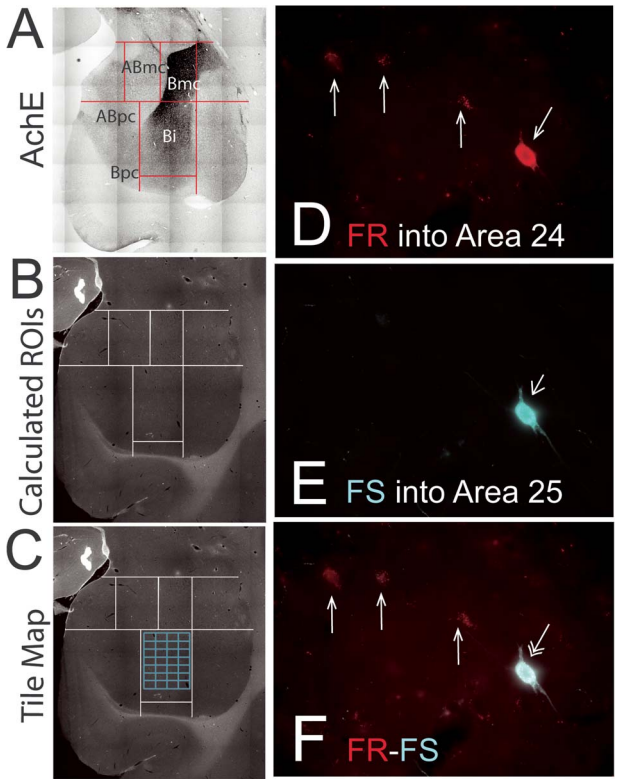

Figure 5 . Double fluorescence microscopy of the amygdala to identify collateral projections. (*A*) Neighboring acetylcholinesterase-stained sections were used to visualize amygdala subnuclei boundaries (boundaries marked in red). (*B*) ROIs created for analysis included the Bmc, Bi, and ABmc (translated from AChE in [*A*]; see Supplementary Figure S1 for anatomical reference) and applied to neighboring fluorescent section. Any cell found in the Bmc was combined with Bi because a clear majority was at the junction of these two regions. (*C*) Representative example of a tile scan (in blue) for a single ROI, whereby a 20× acquisition through the z-plane of the slice was acquired for the entire ROI for each channel. Briefly, compiled tile scans for each ROI were produced for 2 fluorescence channels, 1 for the channel corresponding to the tracer from the pgACC and another, independently, for the sgACC tracer channel. (*D–F*) Immunofluorescent analysis of Fluoro-ruby (FR) (large white arrow, *D*; injected into area 24), Fluorescein (FS) (small white arrow, *E*; injected into area 25), and dual-labeled cells (double arrow head, *F*). Cells were first independently identified in each channel, and then the channels were combined (*F*) to identify cells that had taken up tracers from both the pgACC and sgACC. All cells identified as collateral projections (having taken up both tracers) were confirmed using depth scanning through the z plane to ensure that only a single cell was identified at a position.

double-labeled cells in the Bi projecting to both area 24b/32 and area 25/14c (9.08%, 9.98 mean cell count per injection, two-way ANOVA with Tukey's multiple comparisons post hoc analysis, $df = 30$, $P < 0.0001$). Similarly, a significantly greater proportion of single-labeled cells in ABmc were found following injections in area 25/14c (72.48%, 78.59 mean cell count per injection; Fig. 6C), when compared with the injections in area 24b/32 (19.74%, 38.62 mean cell count per injection; Fig. 6D). There was a small proportion of double-labeled cells in the ABmc as well (7.78%, 8.4 mean cell count per injection, two-way ANOVA with Tukey's multiple comparisons post hoc analysis, $df = 30$, $P < 0.0001$).

We then compared the proportion of single- versus double-labeled neurons in terms of projection paths for the Bi (Fig. 6E) and ABmc (Fig. 6F). In the Bi, a similar percentage of single-labeled cells and double-labeled cells resulted after either area 25/14c or area 24b/32 injections (Fig. 6E; area 25/14c: 86.01% single, 13.99% double; area 24b/32: 79.46% single, 20.54% double). This suggests that a similar proportion of "collateralized" versus "non-collateralized" neurons in the Bi influence the sgACC and pgACC. In contrast, in the ABmc, the proportion of single- and double-labeled cells in each path was different. Single-labeled cells versus double-labeled cells projecting to area 25/14c were 90.31% and 9.69%, respectively. In contrast, single-labeled cells versus double-labeled cells projecting to area 24b/32 were 71.74% and 28.26%, respectively. Therefore, collateral projections from the ABmc represented twice the proportion of total projections to the pgACC compared with the sgACC (Fig. 6F; 28.26% vs. 9.69%). These results indicate a different proportion of neurons projecting from the ABmc are collateralized, depending on the projection target.

Discussion

By using small focused injections, we have found that amygdala inputs to the sgACC and pgACC from the amygdala are surprisingly restricted in the macaque, deriving from the ABmc and Bi almost exclusively. Previous studies using relatively large anterograde injections into the primate amygdala established that the basal nucleus and ABmc project to the ACC (Amaral and Price 1984; Barbas and de Olmos 1990; Aggleton et al. 2015). Moreover, various studies with single retrograde injections into areas 14c, 25, 24, and 32 show labeled cells in Bi and ABmc (Barbas and de Olmos 1990; Carmichael and Price 1996; Ghashghaei and Barbas 2002). Our utilization of multiple paired small volume injections in the areas 25/14c (sgACC) and 24/32 (pgACC) revealed that inputs from both the Bi and ABmc decrease progressively along the caudal–rostral plane of the ACC, a pattern that correlates with the general progression of laminar development in the cortex (Dombrowski et al. 2001; Ongur et al. 2003; Wise 2008). Previous studies have shown this projection trend qualitatively (Amaral and Price 1984; Barbas and de Olmos 1990; Carmichael and Price 1996), and we confirmed it quantitatively. Within this topography, the sgACC, relative to the pgACC, receives greater input from the Bi and ABmc overall and receives a relatively higher proportion of input from the ABmc (Fig.7). Thus, while both the ABmc and Bi project throughout the sgACC and pgACC, there is a shift in combined inputs across regions, with ABmc projections contributing relatively more input to the sgACC compared with the pgACC (see Discussion below).

Comparison with Rodent Studies

These findings agree with rodent studies in a general way, but important differences are noted. Most rodent models examining conditioned fear and extinction responses have focused almost exclusively on IL and PL connections with the BLA (homolog of the primate basal nucleus) (although see Adhikari et al. 2015). IL and/or PL retrograde injections often result in homogeneously and densely distributed labeled cells through the entire BLA (Matyas et al. 2014; Senn et al. 2014), leading to the impression of a nonspecific projection from the entire nucleus. Several studies however show more specific localization of BLA-labeled cells after IL injections, more in line with the present results in the macaque (Kim et al. 2016; Reppucci and Petrovich 2016). Combined injections in the rodent IL and PL appear to result in labeled cells that are intermingled in the BLA (Matyas et al. 2014; Senn et al. 2014). This aligns with the intermingling of sgACC and

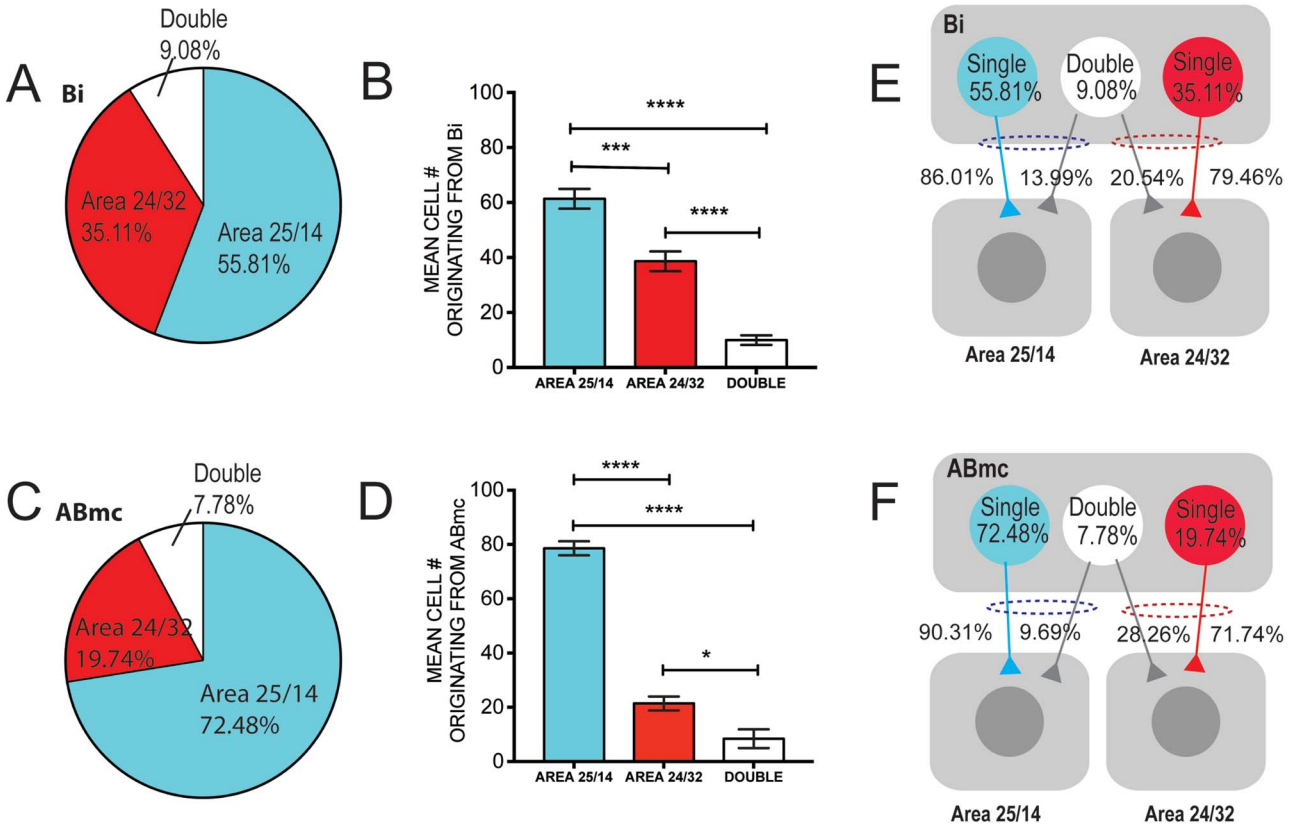

Figure 6. Analysis of projections from the Bi and ABmc to the pgACC and sgACC. Cell counts of tiles scans from Figure 5 revealed proportions of cells from each amygdala sub-nuclei projecting to area 25/14c (sgACC), area 24b/32 (pgACC), or both regions. (*A*,*C*) The proportion of cells labeled with the tracer from area 25/14c, area 24b/32, or double labeled for both tracers in either Bi or ABmc across all cases. Pie charts represent proportions within the pool of all retrogradely labeled cells, across cases, found in the Bi or ABmc. (*B*,*D*) The mean number of cells counted in either Bi or ABmc for each injection identified as single labeled from area 25/14c (blue), single labeled from area 24b/32 (red), or double labeled from both areas (white). (*E*,*F*) Single-pathway analysis, whereby the proportion of single- and double-labeled projections from Bi or ABmc to area 25/14c were compared with those from Bi to area 24b/32. Raw cell counts: injections into area 24/32 = 114 (ABmc), 340 (Bi); injections into area 25/14 = 385 (ABmc), 611 (Bi); double labeled = 46 (ABmc), 83 (Bi). $^{*}P < 0.05$, $^{***}P < 0.005$, $^{****}P < 0.0001$.

pgACC projection neurons in our study, although the combined projection was largely restricted to the Bi, and also importantly included the ABmc.

Adding the ABmc to Fear Circuitry

The ABmc contained labeled cells following all injections in our study. While this region (the BMAp in most rodent studies) is often ignored in studies of fear conditioning and extinction, it projects strongly to the IL (Hoover and Vertes 2007; Reppucci and Petrovich 2016). In the nonhuman primate, ABmc projections have been generally thought to directly mirror basal nucleus projections (Amaral et al. 1992; Schumann et al. 2016). However, our quantification of ABmc and Bi projections reveals that the ABmc has a biased connection with the sgACC as evidenced by the fact that the ABmc sends relatively more projections to the sgACC than the pgACC (Fig. 4C). These trends were confirmed using 2 methods of histochemical staining and analysis in different sections (Fig. 4 and 6, see Discussion below). This bias has also been noted in rats (Petrovich et al. 1996; Reppucci and Petrovich 2016) (see Supplementary Discussion *On Homology between the Primate and Rodent Basal and Accessory Basal Nuclei*).

While most rodent fear extinction studies focus on the role of the basal nucleus (or "BLA"), Adhikari et al. (2015) found that optogenetic activation of the rodent AB (or basomedial/BMA) increased extinction memory strength. The participation of the rodent AB (BMA) in extinction learning may be due to its privileged connections with the IL and also its specific downstream efferents that differ from those of the basal nucleus (Wang et al. 2015; Yamamoto et al. 2018). These functional findings in rodents, combined with data indicating a biased set of projections from the ABmc to the sgACC in monkey (Amaral and Price 1984; Figs 4C and 6C, *D*, and *F*), suggest a unique role for the ABmc in fear extinction and encourage investigation of human prefrontal connections with the AB in fear circuitry.

Are There Correlates of the Infralimbic and Prelimbic Cortices in Primates?

Primate area 25 and IL share various cytoarchitectural (Brodmann 1909; Garey 2006), connectional (Barbas et al. 2003; Heilbronner et al. 2016), and functional (Phelps et al. 2004; Vidal-Gonzalez et al. 2006; Burgos-Robles et al. 2007; Etkin et al. 2011; Sierra-Mercado et al. 2011) features, supporting homology between the 2 regions (see Supplementary Discussion). Macaque sgACC (areas 25 and 14c) is further distinguished from pgACC (areas 32 and 24) by relatively greater inputs from the amygdala overall. A higher proportion of ABmc inputs (Figs 4C and 6) mirrors findings in rodents (Petrovich et al. 1996; Reppucci and Petrovich 2016) and provides more connectional evidence

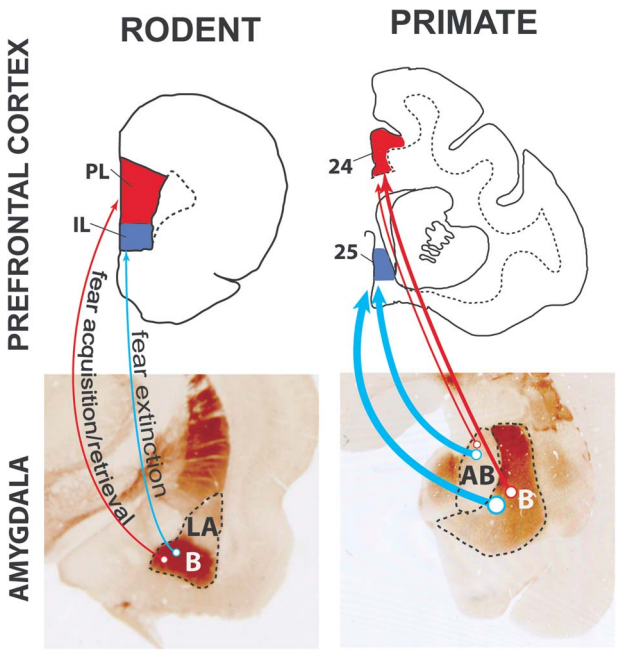

Figure 7. Analogous circuitry for fear acquisition and extinction between rodents and primates. In rodent models, connections between the basal nucleus (B, also referred to as the basolateral nucleus or BLA) and IL are thought to mediate fear extinction while basal to prelimbic (PL) connections mediate fear acquisition and retrieval (expression of fear). In the monkey, area 25/14c is thought to be homologous to the rodent IL and 24/32 to the rodent PL. Connections from the amygdala to these regions originate in both the monkey basal nucleus (B) and the ABmc, which both project to both areas 25/14c (sgACC) and 24/32 (pgACC). A subset of these neurons project collaterally to sgACC and pgACC. Line thickness in the "primate" panels denotes relative projection density from the AB or Bi as detailed in this report. This is the putative circuitry in the nonhuman primate that may parallel fear-learning circuitry in rodents. Findings denote both similarities and interesting differences to the current rodent model. 24: Brodmann area 24. 25: Brodmann area 25. AB: accessory basal nucleus of the amygdala. B: basal nucleus of the amygdala. IL: infralimbic cortex. LA: lateral nucleus of the amygdala. PL: prelimbic cortex.

of homology with the IL. In cross-species studies using monkeys and humans to identify connectional "fingerprints" with resting-state functional magnetic resonance imaging and diffusion-weighted tractography, the sgACC is easily distinguished from nearby regions by relatively stronger links with the ventral tegmental area, ventral striatum, and amygdala (Neubert et al. 2015, Fig. 2E).

There is less agreement regarding the human correlate of the PL. Despite confusion in the nomenclature (see Supplementary Discussion) and Brodmann's specific use of "prelimbic" to avoid claims of homology between area 32 and PL (Brodmann 1909; Garey 2006; Vogt et al. 2013), there is some support for homologies between the rodent PL and the less differentiated portions of primate area 32, located more caudally and ventrally in the medial wall (Vogt et al. 2013). Our connectivity data align with this, as there is greater connectional similarity between more caudal and ventral aspects of the pgACC and rodent PL, consistent with established general trends (Cho YT et al. 2013; Beul et al. 2017). Caudal injections sites in area 32/24 (agranular and dysgranular regions) showed higher connectivity with amygdala, while injections in the rostral portion of area 32 and area 10 (granular regions) showed minimal connectivity with the amygdala (Fig. 4A and B).

These results also correspond with human–monkey connectional "fingerprinting" studies, and their interpretation relies heavily on reward and conflict learning data in primates (Neubert et al. 2015, Figs 2A and 3C and Supplementary Figure 1, respectively). In these studies, caudal pgACC seeds and networks correlate best with human and monkey studies of cost-benefit ("conflict") behavior. Furthermore, human studies of fear learning show that fear appraisal and expression also result in activations over the caudal pgACC as it encircles the corpus callosum (Milad et al. 2007a; Etkin et al. 2011). Our data indicate that these regions best correspond to the caudal, primitive regions in both areas 32 and 24 that receive relatively more amygdala input. Interestingly, area 32 as a whole is a prefrontal hub in primates (Yeterian et al. 2012), with caudal area 32 connecting relatively more primitive cortical regions such as area 25, and more rostral area 32, which receives the least amygdala inputs, linking to the highly developed isocortex (e.g. dorsolateral prefrontal cortex, areas 9 and 46), the latter of which have no clear rodent counterparts (Dombrowski et al. 2001; Ongur et al. 2003; Wise 2008).

sgACC and pgACC Function

The sgACC and pgACC are increasingly recognized to participate in diverse, overlapping networks (Johansen-Berg et al. 2008; Kolling and Rushworth 2015; Neubert et al. 2015). Both areas are interconnected with the amygdala, specifically the basal and ABmc. Understanding the functions of sgACC, pgACC, and the amygdala is challenging, due to the interdependence of these regions and also their likely role in managing the timing, updating, and degree of motivated behaviors (Pare and Quirk 2017; Alexander et al. 2018). In studying such complex behaviors, methods that substantially "drive" or ablate the sgACC or pgACC may obscure function. For example, lesions of sgACC in monkeys decrease the ability to sustain anticipation of future reward (Rudebeck et al. 2014). Oddly, overactivation of sgACC is also linked to loss of anticipation to reward, based on findings in individuals with major depressive disorder (Drevets et al. 1997; Mayberg et al. 1999). Interventions such as deep brain stimulation of the white matter just beneath the sgACC in depressed individuals can reduce sgACC overactivity and restore motivation (presumably by regulating sgACC inflow or outflow) (Mayberg et al. 2005). Consistent with this, over-stimulation of the sgACC in monkeys also blunts anticipatory responses to reward cues (Alexander et al. 2018). This same overstimulation paradigm, however, results in increased arousal to threat; conversely, sgACC inhibition reduces arousal to threat (Wallis et al. 2017).

One interpretation of the above conflicting results is that "driving" the sgACC or ablating it obscures the possibility that it forms a dynamic "rheostat" for detecting and interpreting arousing or salient stimuli based on the animal's moment-to-moment comparisons. Furthermore, the "arousing" features of threat versus reward may also be a confounding factor. Ethologically, threats are frequently more arousing than rewards (for species survival). Thus, maximal activity of the sgACC might be expected to code "threat", whereas lesser activations permit detection of future reward and/or lowered threat along a continuum of experience. Thus, sgACC "hyperactivation" may bias the animal to threat anticipation, disallowing responses to reward anticipation (which would be irrelevant in the face of high threat).

The idea that sgACC activity is critical for fear extinction also appears at odds with the above primate work (Wallis et al. 2017; Alexander et al. 2018). Is this a true species difference or better explained by the sgACC's role in tracking arousal states (Vidal–Gonzalez et al. 2006; Sierra-Mercado et al. 2011; Cho JH et al. 2013; Senn et al. 2014)? Extinction learning requires the animal to move from a highly aroused (threat) state, to a neutral one as it learns that a feared stimulus has lost its salience. Human studies elegantly demonstrate this dynamic, showing that skin conduction responses (and elevated sgACC activity) early in training (when the animal is most fearful) predict reduced amygdala activity by the end of training (Phelps et al. 2004; Schiller et al. 2013).

Key work in awake, behaving monkeys and humans indicates that the pgACC is also involved in flexibly interpreting unexpected cues, or "conflicting" cues, to guide ongoing behavior (Tom et al. 2007; Seo and Lee 2009; Amemori and Graybiel 2012; Kolling et al. 2016). A recent reversal-learning paradigm in awake, behaving monkeys highlights the dynamic nature of pgACC and amygdala interactions in learning about cues. Simultaneous recordings in monkey pgACC (area 24b) and amygdala (basal nucleus) showed that a "surprise" outcome is first detected by the amygdala, then coded in the pgACC (i.e. safer than expected or more aversive than expected), and fed-back to influence later-stage neuron firing in the amygdala neurons (Klavir et al. 2013). This suggests a feed-forward "teaching" loop through amygdala–pgACC–amygdala connections. A separate study that ablated the pgACC supports these results. Ablation of areas 32, 24a, and 24b blocked animals' ability to make use of a "surprise" cue in an appetitive reversal-learning task, suggesting that disconnection of feedback paths to the amygdala disrupts learning about "better than expected" or "worse than expected" cues to guide behavior (Chudasama et al. 2013).

Implications of Collateral Projections

Our tracing results indicate that sgACC and pgACC function in primates likely depends on a precise balance of inputs from the ABmc and Bi to each area (Fig.7). Further supporting the idea of an anatomic substrate for balancing sgACC and pgACC activity, there was a subset of amygdala projections to each region that was collateralized. Although recent models suggest that amygdala inputs to the IL and PL are segregated (Senn et al. 2014), there are abundant examples of collateral long-range projections in the rodent (Sarter and Markowitsch 1984; Reichard et al. 2017; Beyeler et al. 2018; Han et al. 2018; Yamashita et al. 2018) and primate (Rockland 2013) brain. In our primate study, which relied on traditional retrograde techniques, 7.8–9.1% of projections from the amygdala to the pgACC and sgACC were collateral projections to both regions. Our very small injections in widely separated cortical regions make this likely to be a significant underestimation. The area where there was uptake of tracer was limited and would have only labeled a portion of the axonal arbor in each region (Rockland 2013). This is an inherent limitation when working in large brains with large terminal arborizations, such as the primate. We confirmed that AB projections are biased toward sgACC (Fig. 6D and F). We also found that within the smaller set of AB projections to the pgACC, a relatively larger portion of these are collateral projections (28% to pgACC vs. 10% to sgACC; Fig. 6F), suggesting that information in the AB–sgACC path also influences the pgACC. These findings provide evidence that the AB connection is a unique aspect of amygdala–ACC connectivity and that some forms of regulation of both pgACC and sgACC may stem from this region.

Collateralization can promote synchronized neural activity across regions, thereby routing the transmission of relevant information to multiple network areas (Cho et al. 2011; Ciocchi et al. 2015; Kim and Cho 2017). In rodents, synchronized activity between the ACC, amygdala, and hippocampus has been implicated in conditioned fear responses (Lesting et al. 2011). *In vivo* recordings of collateral projections from the ventral hippocampus to the ACC, amygdala, and nucleus accumbens revealed that single, double, and triple projections funneled behavior-specific activity to distinct targets (Ciocchi et al. 2015). In another study using *in vivo* and *ex vivo* optogenetics, ventral hippocampal collateral projections to the amygdala and ACC induced excitatory postsynaptic responses in both regions, with a greater response in the PL versus the IL (Kim and Cho 2017). Thus, collaterals from the hippocampus may specifically facilitate contextual fear responses by activating the PL more robustly than IL to generate a shift in the balance between the PL/IL functional pathways (Quirk and Mueller 2008; Senn et al. 2014). Collateral projections from the amygdala to the IL and PL have not been studied to the same degree, but one question is whether collateral amygdala projections similarly fire to shift the balance between in fear learning and extinction.

Conclusion

Our use of paired injections across the pgACC and sgACC allowed us to investigate the topography and collateral projections of amygdala inputs to a majority of the rostral ACC in nonhuman primates. We found a specific projection to areas 25, 14c, 32, and 24b originating mainly from the Bi and the ABmc. Projection neurons to the sgACC and pgACC were intermingled in each nuclear region. Both the Bi and ABmc project to the sgACC and pgACC but with important differences in the strength of the overall projection, its rostrocaudal topography, and the relative proportion of input from each subnucleus. Functionally, the relative strength of amygdala subcircuits to the sgACC and pgACC may support integrative information flow to guide ongoing learning. In further support of this idea, we found that a small but significant percentage (7.8–9.1%) of projections from the amygdala to the rostral anterior cingulate collaterally project to both the sgACC and pgACC. The specific circuitry connecting these structures in higher species is relevant to elucidating the human correlates of fear circuitry discovered in rodent models.

Funding

National Institute of Mental Health (R01 MH105624 to J.L.F.)

Notes

We thank Ms Nanette Alcock for histologic support. *Conflict of Interest:* None declared.

References

Adhikari A, Lerner TN, Finkelstein J, Pak S, Jennings JH, Davidson TJ, Ferenczi E, Gunaydin LA, Mirzabekov JJ, Ye L *et al.* 2015. Basomedial amygdala mediates top-down control of anxiety and fear. *Nature*. 527:179–185.

Aggleton JP, Wright NF, Rosene DL, Saunders RC. 2015. Complementary patterns of direct amygdala and hippocampal

projections to the macaque prefrontal cortex. *Cereb Cortex*. 25:4351–4373.

Alexander L, Gaskin PLR, Sawiak SJ, Fryer TD, Hong YT, Cockcroft GJ, Clarke HF, Roberts AC. 2018. Fractionating blunted reward processing characteristic of anhedonia by over-activating primate subgenual anterior cingulate cortex. *Neuron*. 101:307–320.

Amaral DG, Price JL. 1984. Amygdalo-cortical projections in the monkey *(Macaca fascicularis)*. *J Comp Neurol*. 230:465–496.

Amaral DG, Price JL, Pitkanen A, Carmichael ST. 1992. Anatomical organization of the primate amygdaloid complex. In: *The amygdala: neurobiological aspects of emotion, memory, and mental dysfunction*. New York: Wiley-Liss, Inc., pp. 1–66.

Amemori K, Graybiel AM. 2012. Localized microstimulation of primate pregenual cingulate cortex induces negative decision-making. *Nat Neurosci*. 15:776–785.

Barbas H, de Olmos J. 1990. Projections from the amygdala to basoventral and mediodorsal prefrontal regions in the rhesus monkey. *J Comp Neurol*. 300:549–571.

Barbas H, Saha S, Rempel-Clower N, Ghashghaei T. 2003. Serial pathways from primate prefrontal cortex to autonomic areas may influence emotional expression. *BMC Neurosci*. 4:25.

Beul SF, Barbas H, Hilgetag CC. 2017. A predictive structural model of the primate connectome. *Sci Rep*. 7:43176.

Beyeler A, Chang CJ, Silvestre M, Leveque C, Namburi P, Wildes CP, Tye KM. 2018. Organization of valence-encoding and projection-defined neurons in the basolateral amygdala. *Cell Rep*. 22:905–918.

Brodmann K. 1909. *"Vergleichende lokalisationslehre der grosshirnrinde" (Comparitive localization theory of the cerebral cortex: illustrated in its principles on the basis of cell construction)*. Leipzig (Germany): J.A. Barth.

Burgos-Robles A, Kimchi EY, Izadmehr EM, Porzenheim MJ, Ramos-Guasp WA, Nieh EH, Felix-Ortiz AC, Namburi P, Leppla CA, Presbrey KN *et al*. 2017. Amygdala inputs to prefrontal cortex guide behavior amid conflicting cues of reward and punishment. *Nat Neurosci*. 20:824–835.

Burgos-Robles A, Vidal-Gonzalez I, Quirk GJ. 2009. Sustained conditioned responses in prelimbic prefrontal neurons are correlated with fear expression and extinction failure. *J Neurosci*. 29:8474–8482.

Burgos-Robles A, Vidal-Gonzalez I, Santini E, Quirk GJ. 2007. Consolidation of fear extinction requires NMDA receptor-dependent bursting in the ventromedial prefrontal cortex. *Neuron*. 53:871–880.

Carmichael ST, Price JL. 1996. Limbic connections of the orbital and medial prefrontal cortex in macaque monkeys. *J Comp Neurol*. 363:615–641.

Cho JH, Bayazitov IT, Meloni EG, Myers KM, Carlezon WA Jr, Zakharenko SS, Bolshakov VY. 2011. Coactivation of thalamic and cortical pathways induces input timing-dependent plasticity in amygdala. *Nat Neurosci*. 15:113–122.

Cho JH, Deisseroth K, Bolshakov VY. 2013. Synaptic encoding of fear extinction in mPFC-amygdala circuits. *Neuron*. 80:1491–1507.

Cho YT, Ernst M, Fudge JL. 2013. Cortico-amygdala-striatal circuits are organized as hierarchical subsystems through the primate amygdala. *J Neurosci*. 33:14017–14030.

Chudasama Y, Daniels TE, Gorrin DP, Rhodes SE, Rudebeck PH, Murray EA. 2013. The role of the anterior cingulate cortex in choices based on reward value and reward contingency. *Cereb Cortex*. 23:2884–2898.

Ciocchi S, Passecker J, Malagon-Vina H, Mikus N, Klausberger T. 2015. Brain computation. Selective information routing by ventral hippocampal CA1 projection neurons. *Science*. 348:560–563.

Dombrowski SM, Hilgetag CC, Barbas H. 2001. Quantitative architecture distinguishes prefrontal cortical systems in the rhesus monkey. *Cereb Cortex*. 11:975–988.

Drevets WC, Price JL, Simpson JR Jr, Todd RD, Reich T, Vannier M, Raichle ME. 1997. Subgenual prefrontal cortex abnormalities in mood disorders. *Nature*. 386:824–827.

Etkin A, Egner T, Kalisch R. 2011. Emotional processing in anterior cingulate and medial prefrontal cortex. *Trends Cogn Sci*. 15:85–93.

Garey LJ. 2006. *Brodmann's localisation in the cerebral cortex*. 3rd ed. New York: Springer.

Ghashghaei HT, Barbas H. 2002. Pathways for emotion: interactions of prefrontal and anterior temporal pathways in the amygdala of the rhesus monkey. *Neuroscience*. 115:1261–1279.

Giustino TF, Maren S. 2015. The role of the medial prefrontal cortex in the conditioning and extinction of fear. *Front Behav Neurosci*. 9:298.

Han Y, Kebschull JM, Campbell RAA, Cowan D, Imhof F, Zador AM, Mrsic-Flogel TD. 2018. The logic of single-cell projections from visual cortex. *Nature*. 556:51–56.

Heilbronner SR, Rodriguez-Romaguera J, Quirk GJ, Groenewegen HJ, Haber SN. 2016. Circuit-based corticostriatal homologies between rat and primate. *Biol Psychiatry*. 80:509–521.

Hoover WB, Vertes RP. 2007. Anatomical analysis of afferent projections to the medial prefrontal cortex in the rat. *Brain Struct Funct*. 212:149–179.

Johansen-Berg H, Gutman DA, Behrens TE, Matthews PM, Rushworth MF, Katz E, Lozano AM, Mayberg HS. 2008. Anatomical connectivity of the subgenual cingulate region targeted with deep brain stimulation for treatment-resistant depression. *Cereb Cortex*. 18:1374–1383.

Kim J, Pignatelli M, Xu S, Itohara S, Tonegawa S. 2016. Antagonistic negative and positive neurons of the basolateral amygdala. *Nat Neurosci*. 19:1636–1646.

Kim WB, Cho JH. 2017. Synaptic targeting of double-projecting ventral CA1 hippocampal neurons to the medial prefrontal cortex and basal amygdala. *J Neurosci*. 37:4868–4882.

Klavir O, Genud-Gabai R, Paz R. 2013. Functional connectivity between amygdala and cingulate cortex for adaptive aversive learning. *Neuron*. 80:1290–1300.

Klavir O, Prigge M, Sarel A, Paz R, Yizhar O. 2017. Manipulating fear associations via optogenetic modulation of amygdala inputs to prefrontal cortex. *Nat Neurosci*. 20:836–844.

Kolling N, Rushworth MF. 2015. What's worth the risk? A neural circuit for trade-offs. *Cell*. 161:1243–1244.

Kolling N, Wittmann MK, Behrens TE, Boorman ED, Mars RB, Rushworth MF. 2016. Value, search, persistence and model updating in anterior cingulate cortex. *Nat Neurosci*. 19:1280–1285.

Krettek JE, Price JL. 1977. Projections from the amygdaloid complex to the cerebral cortex and thalamus in the rat and cat. *J Comp Neurol*. 172:687–722.

Krettek JE, Price JL. 1978. A description of the amygdaloid complex in the rat and cat with observations on intra-amygdaloid axonal connections. *J Comp Neurol*. 178:255–280.

Lesting J, Narayanan RT, Kluge C, Sangha S, Seidenbecher T, Pape HC. 2011. Patterns of coupled theta activity in amygdala–hippocampal–prefrontal cortical circuits during fear extinction. *PLoS One*. 6:e21714.

Likhtik E, Paz R. 2015. Amygdala–prefrontal interactions in (mal)adaptive learning. *Trends Neurosci*. 38:158–166.

Marek R, Xu L, Sullivan RKP, Sah P. 2018. Excitatory connections between the prelimbic and infralimbic medial prefrontal cortex show a role for the prelimbic cortex in fear extinction. *Nat Neurosci*. 21:654–658.

Maren S, Quirk GJ. 2004. Neuronal signalling of fear memory. *Nat Rev Neurosci*. 5:844–852.

Matyas F, Lee J, Shin HS, Acsady L. 2014. The fear circuit of the mouse forebrain: connections between the mediodorsal thalamus, frontal cortices and basolateral amygdala. *Eur J Neurosci*. 39:1810–1823.

Mayberg HS, Liotti M, Brannan SK, McGinnis S, Mahurin RK, Jerabek PA, Silva JA, Tekell JL, Martin CC, Lancaster JL *et al*. 1999. Reciprocal limbic-cortical function and negative mood: converging PET findings in depression and normal sadness. *Am J Psychiatry*. 156:675–682.

Mayberg HS, Lozano AM, Voon V, McNeely HE, Seminowicz D, Hamani C, Schwalb JM, Kennedy SH. 2005. Deep brain stimulation for treatment-resistant depression. *Neuron*. 45:651–660.

McDonald AJ. 1991a. Organization of amygdaloid projections to the prefrontal cortex and associated striatum in the rat. *Neuroscience*. 44:1–14.

McDonald AJ. 1991b. Topographical organization of amygdaloid projections to the caudatoputamen, nucleus accumbens, and related striatal-like areas of the rat brain. *Neuroscience*. 44(1):15–33.

McDonald AJ. 1998. Cortical pathways to the mammalian amygdala. *Prog Neurobiol*. 55:257–332.

Milad MR, Quirk GJ, Pitman RK, Orr SP, Fischl B, Rauch SL. 2007a. A role for the human dorsal anterior cingulate cortex in fear expression. *Biol Psychiatry*. 62:1191–1194.

Milad MR, Wright CI, Orr SP, Pitman RK, Quirk GJ, Rauch SL. 2007b. Recall of fear extinction in humans activates the ventromedial prefrontal cortex and hippocampus in concert. *Biol Psychiatry*. 62:446–454.

Morecraft RJ, McNeal DW, Stilwell-Morecraft KS, Gedney M, Ge J, Schroeder CM, van Hoesen GW. 2007. Amygdala interconnections with the cingulate motor cortex in the rhesus monkey. *J Comp Neurol*. 500:134–165.

Neubert FX, Mars RB, Sallet J, Rushworth MF. 2015. Connectivity reveals relationship of brain areas for reward-guided learning and decision making in human and monkey frontal cortex. *Proc Natl Acad Sci U S A*. 112:E2695–E2704.

Ongur D, Ferry AT, Price JL. 2003. Architectonic subdivision of the human orbital and medial prefrontal cortex. *J Comp Neurol*. 460:425–449.

Ongur D, Price JL. 2000. The organization of networks within the orbital and medial prefrontal cortex of rats, monkeys and humans. *Cereb Cortex*. 10:206–219.

Pare D, Quirk GJ. 2017. When scientific paradigms lead to tunnel vision: lessons from the study of fear. *NPJ Sci Learn*. 2(6). doi: 10.1038/s41539-017-0007-4.

Petrides M, Tomaiuolo F, Yeterian EH, Pandya DN. 2012. The prefrontal cortex: comparative architectonic organization in the human and the macaque monkey brains. *Cortex*. 48:46–57.

Petrovich GD, Risold PY, Swanson LW. 1996. Organization of projections from the basomedial nucleus of the amygdala: a PHAL study in the rat. *J Comp Neurol*. 374:387–420.

Phelps EA, Delgado MR, Nearing KI, LeDoux JE. 2004. Extinction learning in humans: role of the amygdala and vmPFC. *Neuron*. 43:897–905.

Porrino LJ, Crane AM, Goldman-Rakic PS. 1981. Direct and indirect pathways from the amygdala to the frontal lobe in rhesus monkeys. *J Comp Neurol*. 198:121–136.

Price JL, Russchen FT, Amaral DG. 1987. The limbic region. II. The amygdaloid complex. In: Hokfelt BT, Swanson LW, editors. *Handbook of chemical neuroanatomy*. Amsterdam: Elsevier, pp. 279–381.

Quirk GJ, Mueller D. 2008. Neural mechanisms of extinction learning and retrieval. *Neuropsychopharmacology*. 33:56–72.

Reichard RA, Subramanian S, Desta MT, Sura T, Becker ML, Ghobadi CW, Parsley KP, Zahm DS. 2017. Abundant collateralization of temporal lobe projections to the accumbens, bed nucleus of stria terminalis, central amygdala and lateral septum. *Brain Struct Funct*. 222:1971–1988.

Reppucci CJ, Petrovich GD. 2016. Organization of connections between the amygdala, medial prefrontal cortex, and lateral hypothalamus: a single and double retrograde tracing study in rats. *Brain Struct Funct*. 221:2937–2962.

Rockland KS. 2013. Collateral branching of long-distance cortical projections in monkey. *J Comp Neurol*. 521: 4112–4123.

Rudebeck PH, Putnam PT, Daniels TE, Yang T, Mitz AR, Rhodes SE, Murray EA. 2014. A role for primate subgenual cingulate cortex in sustaining autonomic arousal. *Proc Natl Acad Sci U S A*. 111:5391–5396.

Sarter M, Markowitsch HJ. 1984. Collateral innervation of the medial and lateral prefrontal cortex by amygdaloid, thalamic, and brain-stem neurons. *J Comp Neurol*. 224: 445–460.

Schiller D, Delgado MR. 2010. Overlapping neural systems mediating extinction, reversal and regulation of fear. *Trends Cogn Sci*. 14:268–276.

Schiller D, Kanen JW, LeDoux JE, Monfils MH, Phelps EA. 2013. Extinction during reconsolidation of threat memory diminishes prefrontal cortex involvement. *Proc Natl Acad Sci U S A*. 110:20040–20045.

Schumann CMV, Vargas M, Lee A. 2016. A synopsis of primate amygdala neuroanatomy. In: Amaral DG, Adolphs R, editors. *Living without an amygdala*. New York, London: The Guilford Press, pp. 39–71.

Senn V, Wolff SB, Herry C, Grenier F, Ehrlich I, Grundemann J, Fadok JP, Muller C, Letzkus JJ, Luthi A. 2014. Long-range connectivity defines behavioral specificity of amygdala neurons. *Neuron*. 81:428–437.

Seo H, Lee D. 2009. Behavioral and neural changes after gains and losses of conditioned reinforcers. *J Neurosci*. 29: 3627–3641.

Sesack SR, Deutch AY, Roth RH, Bunney BS. 1989. Topographical organization of the efferent projections of the medial prefrontal cortex in the rat: an anterograde tract-tracing study with Phaseolus vulgaris leucoagglutinin. *J Comp Neurol*. 290:213–242.

Sierra-Mercado D, Padilla-Coreano N, Quirk GJ. 2011. Dissociable roles of prelimbic and infralimbic cortices, ventral hippocampus, and basolateral amygdala in the expression and extinction of conditioned fear. *Neuropsychopharmacology*. 36:529–538.

Stephan H, Frahm HD, Baron G. 1987. Comparison of brain structure volumes in Insectivora and primates VII. Amygdaloid components. *J Hirnforsch*. 5:571–584.

Tom SM, Fox CR, Trepel C, Poldrack RA. 2007. The neural basis of loss aversion in decision-making under risk. *Science*. 315:515–518.

Vidal-Gonzalez I, Vidal-Gonzalez B, Rauch SL, Quirk GJ. 2006. Microstimulation reveals opposing influences of prelimbic and infralimbic cortex on the expression of conditioned fear. *Learn Mem*. 13:728–733.

Vogt BA, Hof PR, Zilles K, Vogt LJ, Herold C, Palomero-Gallagher N. 2013. Cingulate area 32 homologies in mouse, rat, macaque and human: cytoarchitecture and receptor architecture. *J Comp Neurol*. 521:4189–4204.

Vogt BA, Paxinos G. 2014. Cytoarchitecture of mouse and rat cingulate cortex with human homologies. *Brain Struct Funct*. 219:185–192.

Wallis CU, Cardinal RN, Alexander L, Roberts AC, Clarke HF. 2017. Opposing roles of primate areas 25 and 32 and their putative rodent homologs in the regulation of negative emotion. *Proc Natl Acad Sci USA*. 114: E4075–E4084.

Wang L, Chen IZ, Lin D. 2015. Collateral pathways from the ventromedial hypothalamus mediate defensive behaviors. *Neuron*. 85:1344–1358.

Wise SP. 2008. Forward frontal fields: phylogeny and fundamental function. *Trends Neurosci*. 31:599–608.

Yamamoto R, Ahmed N, Ito T, Gungor NZ, Pare D. 2018. Optogenetic study of anterior BNST and basomedial amygdala projections to the ventromedial hypothalamus. *eNeuro*. 5(2). doi: 10.1523/ENEURO.0204-18.2018.

Yamashita T, Vavladeli A, Pala A, Galan K, Crochet S, Petersen SSA, Petersen CCH. 2018. Diverse long-range axonal projections of excitatory layer 2/3 neurons in mouse barrel cortex. *Front Neuroanat*. 12:33.

Yeterian EH, Pandya DN, Tomaiuolo F, Petrides M. 2012. The cortical connectivity of the prefrontal cortex in the monkey brain. *Cortex*. 48:58–81.